Fabrication of a Molecular Self-Assembled Monolayer Diode Using Nanoimprint Lithography

Michael D. Austin* and Stephen Y. Chou

NanoStructure Lab, Department of Electrical Engineering, Princeton University, Princeton, New Jersey 08544

ABSTRACT

We report a simple parallel process for the fabrication of nanoscale electrical contacts to probe the conductance characteristics of a molecular self-assembled monolayer (SAM) using nanoimprint lithography (NIL), a patterning technology capable of sub-10 nm resolution. We fabricated multiple samples, each with 40 gold contacts to a commonly investigated SAM, octadecanethiol (C-18). The contacts were fabricated by growing a SAM on gold nanowire and then patterning a second gold wire over the SAM. The electrical conductivity characteristics of the molecule can be reproduced between samples, suggesting a reliable fabrication process. Our procedure can be employed to study the conductance of any candidate thiol-terminated SAM of interest. Such flexibility permits extensive study of molecular devices and optimization of the processing required to merge silicon with molecular self-assembly.

As semiconductor electronic devices scale down to the sub-10 nm range, there is increasing interest in fabricating devices using molecules that "self-assemble". However, fabricating contacts small enough to probe the electronic characteristics of molecules has proved challenging. Typically, contacts are made one at time with serial processing such as atomic force microscope (AFM) probing,[1] scanning tunneling microscope (STM) probing,[2] electromigration,[3] electrochemical growth,[4] electron beam lithography (EBL),[5,6] trapping colloidal gold particles with dielectric force,[7] or shadow evaporating.[8] Often the electronic characteristics of candidate molecules are unknown, or data obtained from different labs is contradictory. Furthermore, the traditional silicon-based fabrication and patterning techniques are often incompatible with the conditions necessary to self-assemble single molecules. Hence, a simple parallel process that allows for conductance probing of self-assembled molecules is of great interest to further this field, as this would allow for repeatable data collection, and greater opportunity to optimize fabrication processes. Here we present such a process using nanoimprint lithography (NIL), a patterning technology capable of sub-10 nm resolution.[9] To demonstrate the effectiveness of this process, the electronic characteristics of a commonly available molecule, octadecanethiol (C-18), are studied.

Referring to Figure 1, the fabrication process is summarized. On a silicon wafer, a stack of 220 nm low-pressure chemical vapor deposition (LPCVD) silicon nitride (Si_3N_4), 250 nm plasma enhanced chemical vapor deposition (PECVD) silicon dioxide (SiO_2), and 220 nm LPCVD Si_3N_4 was grown. A film of NIL imprint polymer was then spin coated and patterned using an NIL mold in the shape of a nanowire with a 90° angle. The mold was fabricated from a silicon wafer, and was patterned with EBL. The mold was pressed into the NIL polymer heated above its glass transition temperature so the polymer conformed around the mold. The sample was cooled, and then the mold released. The same mold was used in over 50 imprints, with no observable damage or loss in critical dimension control. Detailed information on the NIL process is given elsewhere.[9] NIL rapidly allowed the patterning of 40 samples on the chip surface with the nanowire widths varying from 200 down to 40 nm. Using the NIL polymer as a mask, a CHF_3 reactive ion etch (RIE) was used to etch through the nitride and partially etch through the oxide, producing a trench. The NIL polymer was stripped with acetone, and a wet etch of diluted hydrofluoric (HF) acid was used to etch the oxide, exposing the bottom nitride, and under-etching the top nitride layer by approximately 400 nm as shown in Figure 1c.

The function of the top nitride layer was to provide a shadow mask for the pattering of the gold contacts to the SAM. This allowed patterning without the use of developing or lift-off solvents, which may damage the SAM. To start, 30 nm of gold was evaporated at an angle of 30°, filling one trench as shown in Figure 1d, thus producing a nanowire in the trench. The top nitride mask prevented the gold from entering the second trench. The sample was then moved into a nitrogen glovebox with less than 1 ppm H_2O and O_2

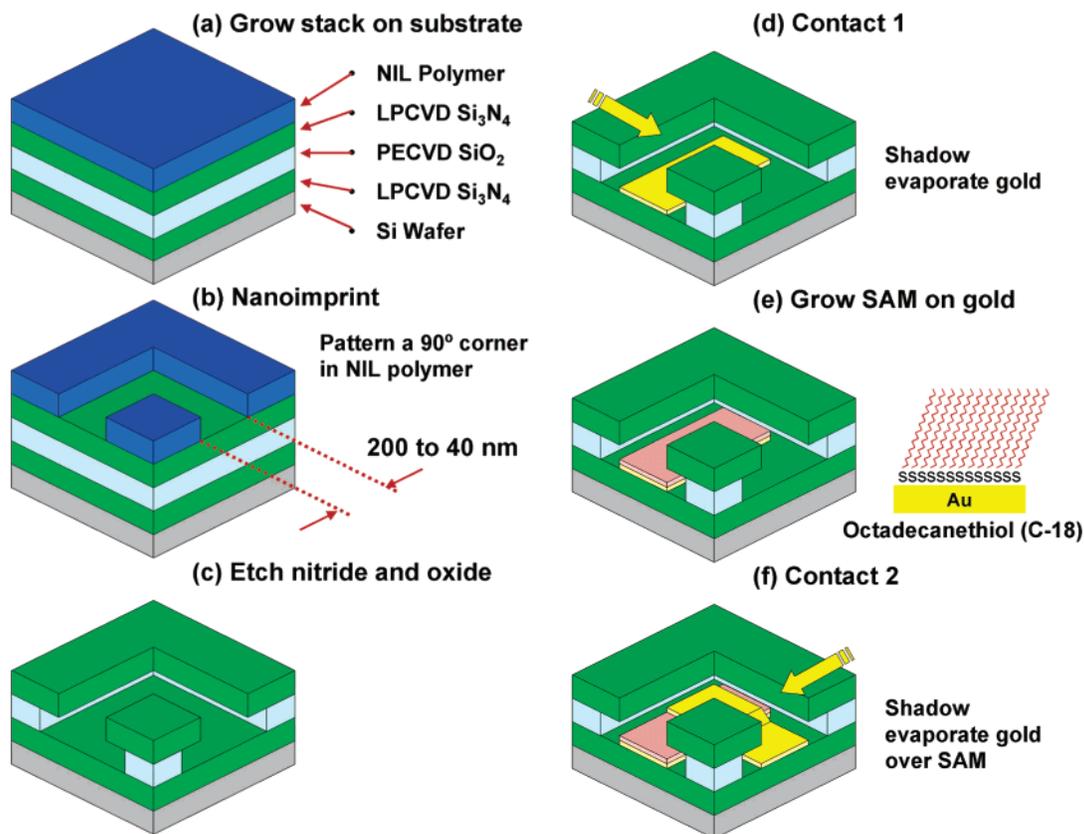* Corresponding author. E-mail: mdaustin@princeton.edu.

Figure 1. Summary of the fabrication process. (a) Initial stack on silicon wafer substrate. (b) Imprint polymer was patterned with nanoimprint lithography (NIL). (c) Reactive ion etching (RIE) etched through the upper silicon nitride layer, and partially through the silicon dioxide to form a trench. A selective hydrofluoric (HF) acid wet silicon dioxide etch was then used to expose the lower nitride layer. (d) Using the top nitride as a shadow mask, gold was evaporated down one trench to form the first contact. (e) A C-18 self-assembled monolayer (SAM) was grown on the gold contact. (f) A second contact to the SAM was produced by evaporating gold down the other trench.

content, and the gold was annealed at 300 °C for 3 h. After annealing, the sample was placed in an ethanol solution of 10 μM C-18, allowing the SAM to grow on the gold nanowire as shown in Figure 1e. After four days of growth, the sample was removed from the solution, rinsed in ethanol, removed from the glovebox, and then immediately placed in an electron beam evaporator vacuum chamber. Again, at an angle of 30° but rotated by 90° with respect to the first gold nanowire, the second contact was made to the SAM by evaporating gold down the second trench as shown in Figure 1f. This step is critical as the gold atoms can damage the monolayer upon impact. To protect the monolayer the evaporation rate was kept at 0.2 Å/s, and the sample was held at −160 °C with a liquid nitrogen cooling stage during the evaporation.[6]

It is critical that the interface between the SAM and the gold atoms be free of contaminants in order to obtain repeatable and reliable SAM $I–V$ characteristics. Unfortunately, the cooling stage acts as a "cold trap" for outgassed particles in the evaporator chamber, thus impurities collect on the SAM surface when the sampled is cooled. To minimize this effect, the evaporation of Au atoms was performed in a vacuum better than 1×10^{-6} Torr, and a condensation shield was employed as shown in Figure 2. The shield was first baked at 200 °C overnight to outgas and then loaded into the evaporation chamber with the
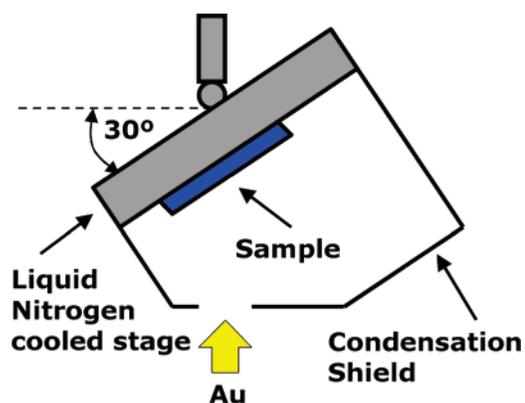

Figure 2. Schematic of the liquid nitrogen stage used to cool the sample to −160 °C during the evaporation of the gold atoms for the second contact to the SAM.

sample. Furthermore, to prevent the gold from peeling off due to thermal stress, the sample was warmed very slowly to room-temperature overnight in a vacuum after evaporation.

The chip with 40 samples of contacts to the C-18 SAM was now complete, with active regions varying from 200 × 200 nm down to 40 × 40 nm. Minimizing the active region area with NIL is key to minimizing the chance of shorts between the contacts via defects in the monolayer.

Using an HP 4145B semiconductor analyzer to probe the monolayer conductivity, most samples showed linear, highly
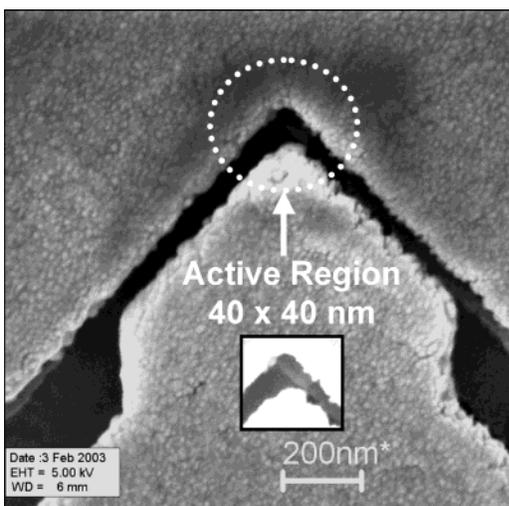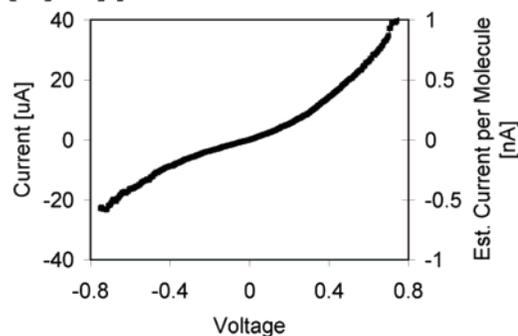
Figure 3. Scanning electron microscope (SEM) image of a finished sample. The inset shows a high contrast image looking down into the trench of the 40×40 nm active region, where the overlapping gold contacts can be seen. Between the overlapping contacts is a C-18 SAM. On each chip, 40 such contacts were fabricated.
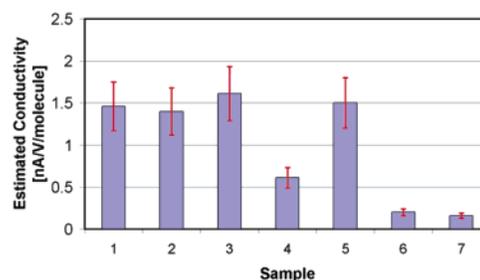

Figure 4. (a) A typical $I-V$ characteristic of a C-18 monolayer. The left axis indicates the measured current vs applied voltage; the right axis is an estimation of current per molecule taking into account the C-18 SAM packing density and active region area. (b) Measured sample conductivities of working samples at 0.5 V that demonstrated repeatable $I-V$ characteristics. Error originates from the measurement of the active region area.

conductive responses, identical to control experiments without a SAM. This suggests that an electric short had occurred, possibly due to a SAM growth defect, or damage to the SAM during the top gold evaporation. However, approximately 5% of the samples appeared to be functional. The voltage was swept in the positive and negative direction, and the current measured. The measured conductivity initially varied, but typically after 10 cycles, the response saturated. Using an SEM to measure the active area of the contact as shown in Figure 3, an estimate can be made as to the conductivity of a single molecule using the well-known packing density of 18.4 Å² per alkanethiol molecule on a Au (111) surface.[10] Figure 4a shows a typical $I-V$ relationship indicating a single molecule resistance of 1800 ± 400 MΩ at 0.1 V, similar to that reported previously with direct AFM measurement of an octanedithiol molecule of 900 MΩ at 0.1 V.[1] Possible explanations for this discrepancy include the longer length of C-18 and the absence of a second thiol group on the end of the molecule, which should reduce the contact resistance between the molecule and top gold contact. Measurements of octanethiol (C-8) SAMs were attempted with this process as well; however, all measured devices shorted. (Measurement of octanedithiol was not attempted as the flexible nature of the alkane chain results in dithiol molecules lying flat, bonding to the gold substrate with both thiols[1,10].)

A comparison among samples that survived measurement long enough to clearly establish saturation and thus repeatable curve traces is shown in Figure 4b, with most measured conductivities around 1.5 nAmp/V/molecule at an applied voltage of 0.5 V. We speculate that the samples with lower conductivities were due to formation of multilayers rather than a monolayer.[10] The samples had limited life spans and would typically short after 30 to 50 cycles, or if more than 1 V was applied. SEM images taken after sample shorts revealed no electromigration damage to the gold nanowires, and the short was irreversible, suggesting that gold atoms

had migrated through the monolayer. Alkanethiol molecules were chosen because they are available commercially and their monolayer preparation has been studied extensively. Unfortunately, alkanethiol molecules consist of a σ-bonded backbone and thus are highly flexible, unlike the rigid backbone of fully conjugated Π-bonded molecules. This flexibility is most likely responsible for the low yields, and the limited life-span of the devices, allowing the gold atoms to easily penetrate the monolayer.

Further decrease in yields may be due to the poor quality of the SAM at the edges of the electrode; however, such limitations are also present in past proposed structures.[5,8] The advantage of this approach to conductivity measurement is full parallel processing of electrodes with sub-100 nm dimensions. In addition, unlike ref 6, this approach does not require etching through the backside of a wafer, thus allowing for greater future circuit integration flexibility.

In conclusion, we have demonstrated a simple structure to study the conductivity properties of a SAM. Although an interesting test example, it is clear that the alkanethiol monolayer is both too conductive and insufficiently robust to be used as an insulator as previously suggested.[11] Regardless, this process can be used to study the potential candidacy of any thiol-based SAM for use in molecular devices. In addition, the small feature size and high-throughput patterning of NIL allows for the generation of multiple samples for investigating and optimizing the merging of traditional silicon processing with molecular self-assembly.

References

(1) Cui, X. D.; Primak, A.; Zarate, X.; Tomfohr, J.; Sankey, O. F.; Moore, A. L.; Moore, T. A.; Gust, D.; Harris, G.; Lindsay, S. M. *Science* **2001**, *294*, 571.
(2) Andres, R. P.; Bein, T.; Dorogi, M.; Feng, S.; Henderson, J. I.; Kubiak, C. P.; Mahoney, W.; Osifchin, R. G.; Reifenberger, R. *Science* **1996**, *272*, 1323.
(3) Park, J.; Pasupathy, A. N.; Goldsmith, J. I.; Chang, C.; Yaish, Y.; Petta, J. R.; Rinkosi, M.; Sethna, J. P.; Abruna, H. D.; McEuen, P. L.; Ralph, D. C. *Nature* **2002**, *417*, 722.
(4) Li, C. Z.; He, H. X.; Bogozi, A.; Bunch, J. S.; Tao, N. J. *Appl. Phys. Lett.* **2000**, *76*, 1333.
(5) Lee, J.; Lientschnig, G.; Wiertz, F.; Struijk, M.; Janssen, R. A. J.; Egberink, R.; Reinhoudt, D. N.; Hadley, P.; Dekker, C. *Nano Lett.* **2003**, *3*, 113.
(6) Chen, J.; Reed, M. A.; Rawlett, A. M.; Tour, J. M. *Science* **1999**, *286*, 1550.
(7) Amlani, I.; Rawlett, A. M.; Nagahara, L. A.; Tsui, R. K. *Appl. Phys. Lett.* **2002**, *80*, 2761.
(8) Kagan, C. R.; Afzali, A.; Martel, R.; Gignac, L. M.; Solomon, P. M.; Schrott, A. G.; Ek, B. *Nano Lett.* **2003**, *3*, 119.
(9) Chou, S. Y.; Krauss, P. R.; Renstrom, P. J. *Science* **1996**, *272*, 85.
(10) Schreiber, F. *Prog. Surf. Sci.* **2000**, *65*, 151.
(11) Schön, J. H.; Bao, Z. *Appl. Phys. Lett.* **2002**, *80*, p 332.

NL034831P